Joint H.E.S.S. and Fermi-LAT analysis of the region around PSR J1813-1749

T. Wach,[a,*] **A. M. W. Mitchell,**[a] **V. Joshi,**[a] **S. Funk**[a] **and on behalf of the H.E.S.S. Collaboration**

[a]*Friedrich-Alexander-Universität Erlangen-Nürnberg, Erlangen Centre for Astroparticle Physics, Nikolaus-Fiebiger-Straße 2, D 91058 Erlangen, Germany*

E-mail: tina.wach@fau.de

HESS J1813-178 is one of the brightest sources detected during the first HESS Galactic Plane survey. The compact source, also detected by MAGIC, is believed to be a pulsar wind nebula powered by one of the most powerful pulsars known in the Galaxy, PSR J1813-1749 with a spin-down luminosity of $\dot{E} = 5.6 \cdot 10^{37} \, \mathrm{erg \, s^{-1}}$. With its extreme physical properties, as well as the pulsar's young age of 5.6 kyrs, the γ-rays detected in this region allow us to study the evolution of a highly atypical system. Previous studies of the region in the GeV energy range show emission extended beyond the size of the compact H.E.S.S. source. Using the archival H.E.S.S. data with improved background methods, we perform a detailed morphological and spectral analysis of the region. Additionally to the compact, bright emission component, we find significantly extended emission, whose position is coincident with HESS J1813-178. We reanalyse the region in GeV and derive a joint-model in order to find a continuous description of the emission in the region from GeV to TeV. Using the results derived in this analysis, as well as X-ray and radio data of the region, we perform multi-wavelength spectral modeling. Possible hadronic or leptonic origins of the γ-ray emission are investigated, and the diffusion parameters necessary to explain the extended emission are examined.

PoS(ICRC2023)589

*Speaker

1. Introduction

The Imaging Atmospheric Cherenkov Telescope (IACT) Array H.E.S.S. has highly contributed to our knowledge of the γ-ray sky, by identifying many previously unknown sources during their surveys of the galactic plane (HGPS) conducted in 2006 [3] and 2018 [12]. One of these sources is HESS J1813−178, a single-component compact source, centered at R.A. = $(273.40 \pm 0.005)°$, Dec = $-(17.84 \pm 0.005)°$ with an extension of $\sigma = (0.036 \pm 0.006)°$. Compact counterparts to this high energy γ-ray emission have been observed in X-ray with INTEGRAL [19] and XMM-Newton [11] and in radio with the VLA [7]. Additionally, faint extended emission enclosing the bright compact emission has been detected during the HGPS in 2006. This detection however could not be established as significant [3].

The detection of the shell-type Supernova Remnant (SNR) G12.82–0.02 [7], and the very young and energetic pulsar PSR J1813−1749, with a characteristic age of 5600 years and a spin-down luminosity of $\dot{E} = 5.6 \times 10^{37}\,\mathrm{ergs}^{-1}$ [8], both positionally coincident with the detected TeV emission, result in two different scenarios for the origin of the γ-ray emission. Several studies showed that it is more likely that the compact γ-ray emission observed in the TeV range is a result of Inverse Compton (IC) scattering of electrons from the pulsar with photons of the ISM [10, 11]

An analysis of the region in the GeV energy range, utilising data taken with the *Fermi*-LAT satellite, showed emission that is positionally coincident with PSR J1813−1749, but extended $(0.6 \pm 0.06)°$ [6]. They concluded that the origin of the TeV and GeV emission should be considered separately, and found that the origin of the γ-ray emission in the GeV energy range is most likely Cosmic Rays (CRs) accelerated at the shock fronts of the SNR. An additional hadronic scenario could be CRs accelerated at the shock fronts of the young stellar cluster Cl J1813−178, located in close proximity to the pulsar as projected along the line of sight [16]. Due to the mismatch in observed emission extension, and the very different interpretation of the data acquired in different energies, the origin of the emission in the region around PSR J1813−1749 could not be firmly established yet.

We present a reanalysis of the TeV data in the region around HESS J1813−178, using improved background rejection and event reconstruction. We also present a new analysis of the *Fermi*-LAT data, with increased exposure compared to the previous work, and perform a joint-likelihood minimisation of the GeV and TeV data simultaneously.

2. H.E.S.S. Data Analysis and Results

H.E.S.S. data is taken in ∼ 28 min observation intervals referred to as runs. We select the runs for this analysis based on requiring that all four telescopes must participate, and the pointing position of the telescopes, which must be less than 2° offset from the position of HESS J1813−178 derived in the previous analysis. Additionally, standard data quality cuts [2] are applied and the energy threshold of the analysis is set to 0.4 TeV. Applying these quality cuts results in a dataset with 31 hours of livetime, taken between 2004 and 2012. We then analyse the data using the open-source Python package `gammapy, version 0.18.2` [9].

The first galactic plane survey [3] was evaluated using the Ring background method. This method estimates the background from source-free regions at equal distance from the source. The
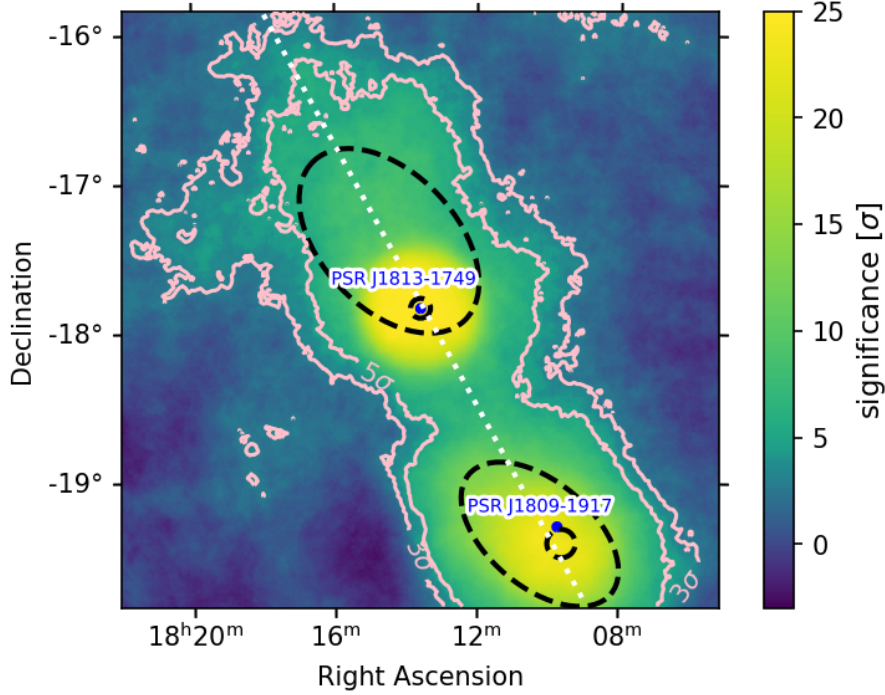
Figure 1: Significance map of the region around PSR J1813−1749 as seen by H.E.S.S. before removal of emission using source models. The galactic plane is indicated by the white dotted line, $3\,\sigma$ and $5\,\sigma$ contours are shown in pink. The best-fit source model for HESS J1809−193 derived in [14] is shown by the black dashed line and the best-fit model for the emission around PSR J1813−1749 derived in this study.

results acquired from this background method depend on a correct estimation of the source extension and is highly sensitive to point-like sources, but not suitable for faint or very extended sources and problematic for sources without a defined edge, like pulsar wind nebulae. In order to increase the sensitivity towards large extended sources, we use a template-based approach to describe the background. This template is generated from a large set of source-free regions, following the scheme in [17].

Figure 1 shows the significance map of the region around HESS J1813−178 with a correlation radius of $0.4°$. The position of the galactic plane is indicated by the white dotted line. We also show $3\,\sigma$ and $5\,\sigma$ contours of the emission, as well as the position of PSR J1813−1749 and PSR J1809−1917, a nearby pulsar enclosed by the TeV source HESS J1809−193. In this analysis, the emission of the neighbouring source HESS J1809−193 is removed by adding a two-component model, following the description derived in a recent analysis of this region [14].

We observe a compact bright emission centered around the pulsar, as well as a fainter, extended emission in the region around the pulsar. We account for the emission around PSR J1813−1749 by adding a Gaussian source model with an extension of $\sigma = 0.056° \pm 0.003°$. The best-fit results derived for this source model agree within the error with the previously results for HESS J1813−178 [3]. Hereafter, we will refer to this emission component as component A. After the removal of this component by modeling the emission, we observe a remaining large-scale γ-ray emission component. We find that this emission can be best described by an asymmetric Gaussian model,
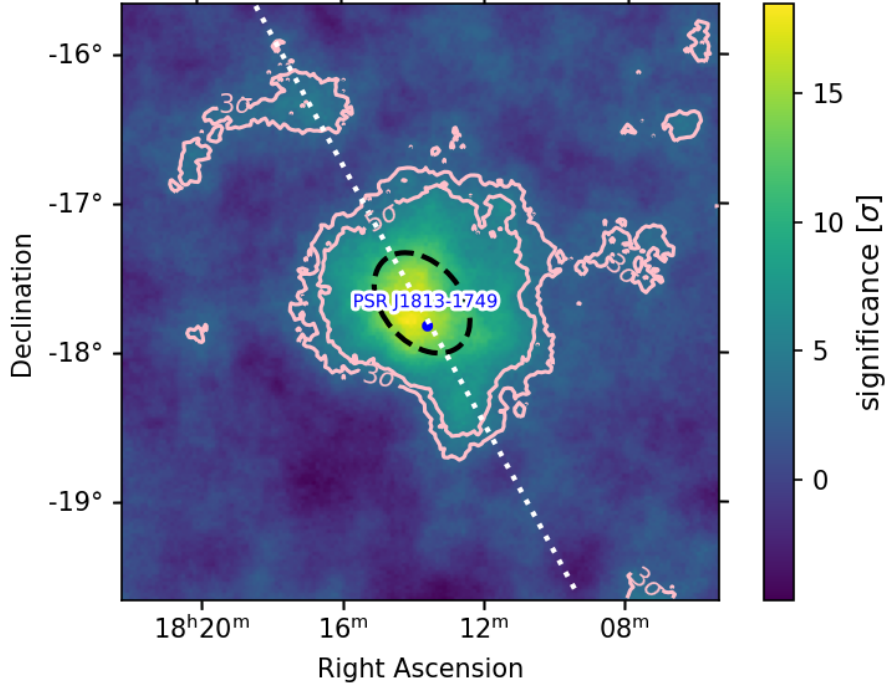
Figure 2: Significance map of the region containing 4FGL J1813−1737e as seen by *Fermi*-LAT. Additional emission in the field of view attributed to other astrophysical sources has been removed using their description in the 4FGL source catalogue. $3\,\sigma$ and $5\,\sigma$ contours of the residual emission in the field of view are overlaid in pink. The best-fit model is for 4FGL J1813−1737e is indicated by the black dashed line

aligned along the galactic plane. We will refer to this source model as component B. The best-fit values for the two source models used to account for the emission around PSR J1813−1749, as well as the source models used to account for the emission in the vicinity of PSR J1809−1917, are indicated by the black dashed lines in figure 1.

3. *Fermi*-LAT Data Analysis and Results

In a previous analysis of the *Fermi*-LAT data of the region around PSR J1813−1749 using the standard LAT analysis software `Fermitools`, extended emission has been discovered [6]. This source, referred to as 4FGL J1813−1737e, is positionally coincident with PSR J1813−1749 and HESS J1813−178, but with an extension of 0.6°, no connection could be made with the TeV emission. We reanalyse the data using `gammapy, version 0.18.2`, which enables us to optimise the morphology and spectrum of a source model simultaneously.

For this study, data from the beginning of the *Fermi*-LAT mission in August 2008 until October 2021 is used. We use the most recent IRFs from Pass 8 version 3 — `P8R3_SOURCE_V2` [4], and the corresponding background models `iso_P8R3_SOURCE_V3_v1.txt`, `gll_iem_v07.fits`. Other sources in the 6° Region-of-Interest (ROI) are accounted for by using source models from the 12-year 4FGL source catalogue [1]. We allow a maximum zenith angle of 90° for all events to avoid the inclusion of secondary γ-rays from the Earth's horizon, and use a bin size of 0.025°, as well as

8 energy bins per decade with logarithmic spacing. In order to avoid a large point-spread function we adopt an energy threshold of 1 GeV up to 1 TeV.

Figure 2 shows the significance map of the region around PSR J1813−1749, as seen by *Fermi*-LAT. The emission from all sources in the ROI, except 4FGL J1813−1737e, has been accounted for by the respective source model in the 4FGL catalog. We again overlay the galactic plane as a white dotted line, the position of PSR J1813−1749, as well as $3\,\sigma$ and $5\,\sigma$ contours of the emission. Similarly to previous analyses of the region [6, 20], we observe extended emission around the pulsar PSR J1813−1749, positionally coincident with HESS J1813−178. In contrast to the previous studies, using a disk model to describe the emission, we find that the emission can be described best by an asymmetric Gaussian model, with an extension of 0.38°, and an alignment along the galactic plane. The best-fit morphology of this model is indicated by the black dashed lines in figure 2.

This emission is positionally coincident with the results derived in the H.E.S.S. data for component B, though less extended. The addition of a second, compact component, coincident with component A in the H.E.S.S. data, improves the description of the region, but cannot be established at a $5\,\sigma$ level and is therefore omitted for this study.

4. Energy-dependent behaviour of the emission

On account of the positional coincidence between the detected γ-ray emission and the pulsar PSR J1813−1749, a leptonic origin of the emission is plausible. Previous studies of such systems have shown an energy-dependent morphology caused by electron diffusion and cooling [13, 15, 18].

Energy band	Energy [GeV]
1	$1.0 - 2.0$
2	$2.0 - 4.0$
3	$4.0 - 7.5$
4	$7.5 - 18$
5	$18 - 58$
6	$58 - 1.0 \times 10^3$
H1	$(0.4 - 1.3) \times 10^3$
H2	$(1.3 - 5.7) \times 10^3$
H3	$(5.7 - 100) \times 10^3$

Table 1: Energy bands used to test for energy-dependent morphology. Fermi bands are shown as 1- 6 and HESS bands as H1-H3
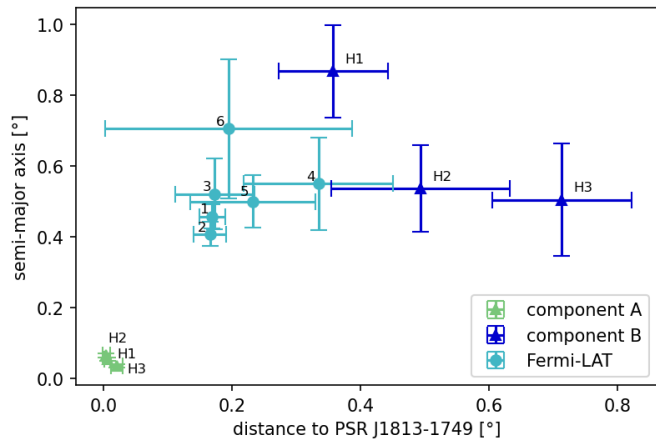

Figure 3: The distance between the centre of the best-fit model and the position of PSR J1813−1749 is estimated in each energy bin and plotted against the extension of the semi-major axis.

To test for an energy-dependent morphology in the emission observed in this study the datasets are divided into six logarithmically spaced energy bins for the *Fermi*-LAT data, as well as three energy bins for the H.E.S.S. data. This binning was chosen based on the available statistics for each dataset. The best-fit models described above are then fitted in each energy bin respectively and the distance of the centre of the best-fit component to the position of PSR J1813−1749 is computed and compared to the extension of the semi-major axis in the respective energy bin. These results are shown in Figure 4.

Due to the low statistics in the H.E.S.S. dataset, as well as the low statistics in the high energy regime of the *Fermi*-LAT dataset, this study is subject to large uncertainties for the respective measurements. The derived extensions are compatible within the errors, we do not find a significant indication of an energy-dependent morphology. However, the extension in the last energy bin of the *Fermi*-LAT data is compatible with the extension derived in the first energy bin of the H.E.S.S. data, suggesting that the emission from 4FGL J1813−1737e can be connected to the extended emission observed in the H.E.S.S. dataset.

5. Joint-Modeling

The discovery of extended emission in the H.E.S.S. data enables a continuous description of the region around PSR J1813−1749, while the search for energy-dependent morphology showed that component B and the extended emission observed in the *Fermi*-LAT data show a comparable extension. To investigate this result, we perform a joint analysis. To describe the emission observed by *Fermi*-LAT and H.E.S.S. we add a symmetric model, as well as an asymmetric model to both datasets. The likelihood minimisation is then performed on both datasets at the same time, while the IRFs for each dataset are taken into account.

This minimisation returns a compact component, centred at a best-fit position of R.A. = $(273.40 \pm 0.003)°$, Dec = $(−17.832 \pm 0.003)°$ with an extension of $\sigma = (0.056 \pm 0.003)°$. Based on the shape of the SED derived in the analysis of the respective datasets, we use a logarithmic parabola spectral model as spectral model. The estimated best-fit spectral index is $\Gamma = 2.05 \pm 0.03$, with a curvature $\beta = 0.06 \pm 0.001$ and a flux normalization at 1 TeV of $(3.16 \pm 0.13) \times 10^{-12}$ cm^{-2}s^{-1}TeV^{-1}.

For the second component, we find a best-fit position of R.A. = $(273.39 \pm 0.03)°$, Dec = $(−17.504 \pm 0.04)°$ with an extension of $\sigma = (0.54 \pm 0.03)°$. This model is asymmetric, with an eccentricity of $e = 0.73 \pm 0.04$ and a position angle of $\varphi = (213.76 \pm 7.22)°$. We again used a logarithmic parabola model with a spectral index of $\Gamma = 2.17 \pm 0.03$, a curvature of $\beta = 0.04 \pm 0.001$, and a flux normalisation at 1 TeV of $(6.47 \pm 0.43) \times 10^{-12}$ cm^{-2}s^{-1}TeV^{-1}.

The spectrum and the spectral energy distribution (SED) for both components can be seen in Figure 4. Additionally, the broadband sensitivity of *Fermi*-LAT for sources located in the galactic plane and 12 years of data taking is overlaid [5]. Most of the predicted emission from component A is below the detectable flux for the LAT, explaining why the emission could not be observed in the analysis of the *Fermi*-LAT data. After removing the emission from components A and B using the best-fit parameters derived in this joint analysis, no emission remains in the H.E.S.S. data. The addition of component A to the *Fermi*-LAT dataset does not overestimate the emission in the region and the significance map is reasonably flat, indicating that this two-component source model is a good description of the region in the GeV and the TeV data.
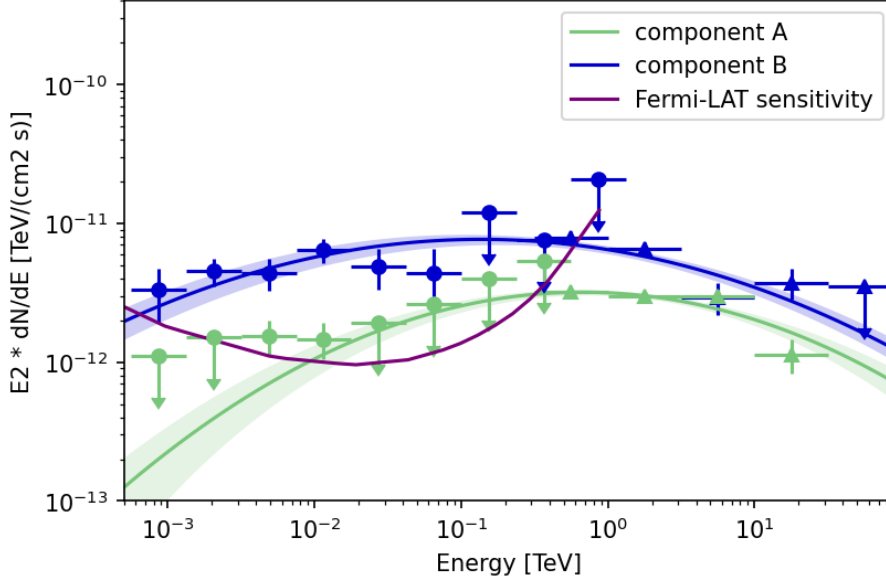
Figure 4: Spectrum and SED for component A and component B derived from a joint-fit to both datasets. The broadband sensitivity of the *Fermi*-LAT is indicated by the purple line [5].

6. Conclusion and Outlook

In previous studies, the emission from HESS J1813−178 and 4FGL J1813−1737e could not be connected, despite their positional coincidence, because of disagreements in the extension measurements. Due to these disagreements, all attempts to draw conclusions on the physical origin of the emission have used either the SED derived in the analysis of the GeV data, or the TeV data separately. As a consequence, the TeV source HESS J1813−178 remains to be a source with an unknown origin.

We reanalyse the region using an improved background model for the analysis of the TeV data, and increased exposure in the GeV data. We find that the emission in the H.E.S.S. data can be well described by a two-component model. The first component, a compact Gaussian component with an extension of 0.06°, referred to as component A in this analysis, can be connected to HESS J1813−178. The detection of a second, extended component in this study makes it possible, for the first time, to connect the emission from 4FGL J1813−1737e to the emission observed in the TeV range and, therefore find a continuous description of the region around PSR J1813−1749 over five decades of energy. Utilising these new results, we will be able to further investigate the physical origin of the emission.

The observed emission is coincident with the pulsar PSR J1813−1749, but also with the SNR G12.82−0.02 and the stellar cluster Cl 1813−178. Therefore the emission could be caused by electrons escaping the confines of the pulsar and forming a pulsar wind nebula, which we would then observe as HESS J1813−178. Some of these electrons further escape into the ISM, forming the halo-like structure observed as 4FGL J1813−1737e and component B. Another possibility is that the observed γ-ray emission is caused by protons from the cosmic ray sea. These protons are accelerated at the shock fronts of the SNR or the stellar cluster. producing γ-rays through

the interaction with photons from molecular clouds in the region. A forthcoming publication will examine these possible emission scenarios in depth and further investigate possible evolution scenarios of the system around PSR J1813−1749.

7. Acknowledgments

Bibliography

[1] Abdollahi, S., Acero, F., Ackermann, M., et al. 2020, , 247, 33

[2] Aharonian, F., Akhperjanian, A. G., Bazer-Bachi, A. R., et al. 2006, , 457, 899

[3] Aharonian, F., Akhperjanian, A. G., Bazer-Bachi, A. R., et al. 2006, , 636, 777

[4] Ajello, M., Atwood, W. B., Axelsson, M., et al. 2021, , 256, 12

[5] Ajello, M., Atwood, W. B., Axelsson, M., et al. 2021, , 256, 12

[6] Araya, M. 2018, , 859, 69

[7] Brogan, C. L., Gaensler, B. M., Gelfand, J. D., et al. 2005, , 629, L105

[8] Camilo, F., Ransom, S. M., Halpern, J. P., & Roshi, D. A. 2021, , 917, 67

[9] Donath, A., Deil, C., Arribas, M. P., et al. 2015, in 34th International Cosmic Ray Conference (ICRC2015), Vol. 34, 789

[10] Fang, J. & Zhang, L. 2010, , 718, 467

[11] Funk, S., Hinton, J. A., Moriguchi, Y., et al. 2007, , 470, 249

[12] H. E. S. S. Collaboration, Abdalla, H., Abramowski, A., et al. 2018, , 612, A1

[13] H. E. S. S. Collaboration, Abdalla, H., Aharonian, F., et al. 2019, , 621, A116

[14] H. E. S. S. Collaboration, Aharonian, F., Ait Benkhali, F., et al. 2023, , 672, A103

[15] MAGIC Collaboration, Acciari, V. A., Ansoldi, S., et al. 2020, , 497, 3734

[16] Messineo, M., Davies, B., Figer, D. F., et al. 2011, , 733, 41

[17] Mohrmann, L., Specovius, A., Tiziani, D., et al. 2019, , 632, A72

[18] Principe, G., Mitchell, A. M. W., Caroff, S., et al. 2020, , 640, A76

[19] Ubertini, P., Bassani, L., Malizia, A., et al. 2005, , 629, L109

[20] Xin, Y. & Guo, X. 2021, PoS, ICRC2021, 625

Full Authors List: H.E.S.S. Collaboration

F. Aharonian[1,2,3], F. Ait Benkhali[4], A. Alkan[5], J. Aschersleben[6], H. Ashkar[7], M. Backes[8,9], A. Baktash[10], V. Barbosa Martins[11], A. Barnacka[12], J. Barnard[13], R. Batzofin[14], Y. Becherini[15,16], G. Beck[17], D. Berge[11,18], K. Bernlöhr[2], B. Bi[19], M. Böttcher[9], C. Boisson[20], J. Bolmont[21], M. de Bony de Lavergne[5], J. Borowska[18], M. Bouyahiaoui[2], F. Bradascio[5], M. Breuhaus[2], R. Brose[1], A. Brown[22], F. Brun[5], B. Bruno[23], T. Bulik[24], C. Burger-Scheidlin[1], T. Bylund[5], F. Cangemi[21], S. Caroff[25], S. Casanova[26], R. Cecil[10], J. Celic[23], M. Cerruti[15], P. Chambery[27], T. Chand[9], S. Chandra[9], A. Chen[17], J. Chibueze[9], O. Chibueze[9], T. Collins[28], G. Cotter[22], P. Cristofari[20], J. Damascene Mbarubucyeye[11], I.D. Davids[8], J. Davies[22], L. de Jonge[9], J. Devin[29], A. Djannati-Ataï[15], J. Djuvsland[2], A. Dmytriiev[9], V. Doroshenko[19], L. Dreyer[9], L. Du Plessis[9], K. Egberts[14], S. Einecke[28], J.-P. Ernenwein[30], S. Fegan[7], K. Feijen[15], G. Fichet de Clairfontaine[20], G. Fontaine[7], F. Lott[8], M. Füßling[11], S. Funk[23], S. Gabici[15], Y.A. Gallant[29], S. Ghafourizadeh[4], G. Giavitto[11], L. Giunti[15,5], D. Glawion[23], J.F. Glicenstein[5], J. Glombitza[23], P. Goswami[15], G. Grolleron[21], M.-H. Grondin[27], L. Haerer[2], S. Hattingh[9], M. Haupt[11], G. Hermann[2], J.A. Hinton[2], W. Hofmann[2], T. L. Holch[11], M. Holler[31], D. Horns[10], Zhiqiu Huang[2], A. Jaitly[11], M. Jamrozy[12], F. Jankowsky[4], A. Jardin-Blicq[27], V. Joshi[23], I. Jung-Richardt[23], E. Kasai[8], K. Katarzyński[32], H. Katjaita[8], D. Khangulyan[33], R. Khatoon[9], B. Khélifi[15], S. Klepser[11], W. Kluźniak[34], Nu. Komin[17], R. Konno[11], K. Kosack[5], D. Kostunin[11], A. Kundu[9], G. Lamanna[25], R.G. Lang[23], S. Le Stum[30], V. Lefranc[5], F. Leitl[23], A. Lemière[15], M. Lemoine-Goumard[27], J.-P. Lenain[21], F. Leuschner[19], A. Luashvili[20], I. Lypova[4], J. Mackey[1], D. Malyshev[19], D. Malyshev[23], V. Marandon[5], A. Marcowith[29], P. Marinos[28], G. Martí-Devesa[31], R. Marx[4], G. Maurin[25], A. Mehta[11], P.J. Meintjes[13], M. Meyer[10], A. Mitchell[23], R. Moderski[34], L. Mohrmann[2], A. Montanari[4], C. Moore[35], E. Moulin[5], T. Murach[11], K. Nakashima[23], M. de Naurois[7], H. Ndiyavala[8,9], J. Niemiec[26], A. Priyana Noel[12], P. O'Brien[35], S. Ohm[11], L. Olivera-Nieto[2], E. de Ona Wilhelmi[11], M. Ostrowski[12], E. Oukacha[15], S. Panny[31], M. Panter[2], R.D. Parsons[18], U. Pensec[21], G. Peron[15], S. Pita[15], V. Poireau[25], D.A. Prokhorov[36], H. Prokoph[11], G. Pühlhofer[19], M. Punch[15], A. Quirrenbach[4], M. Regeard[15], P. Reichherzer[5], A. Reimer[31], O. Reimer[31], I. Reis[5], Q. Remy[2], H. Ren[2], M. Renaud[29], B. Reville[2], F. Rieger[2], G. Roellinghoff[23], E. Rol[36], G. Rowell[28], B. Rudak[34], H. Rueda Ricarte[5], E. Ruiz-Velasco[2], K. Sabri[29], V. Sahakian[37], S. Sailer[2], H. Salzmann[19], D.A. Sanchez[25], A. Santangelo[19], M. Sasaki[23], J. Schäfer[23], F. Schüssler[5], H.M. Schutte[9], M. Senniappan[16], J.N.S. Shapopi[8], S. Shilunga[8], K. Shiningayamwe[8], H. Sol[20], H. Spackman[22], A. Specovius[23], S. Spencer[23], Ł. Stawarz[12], R. Steenkamp[8], C. Stegmann[14,11], S. Steinmassl[2], C. Steppa[14], K. Streil[23], I. Sushch[9], H. Suzuki[38], T. Takahashi[39], T. Tanaka[38], T. Tavernier[5], A.M. Taylor[11], R. Terrier[15], A. Thakur[28], J.H.E. Thiersen[9], C. Thorpe-Morgan[19], M. Tluczykont[10], M. Tsirou[11], N. Tsuji[40], R. Tuffs[2], Y. Uchiyama[33], M. Ullmo[5], T. Unbehaun[23], P. van der Merwe[9], C. van Eldik[23], B. van Soelen[13], G. Vasileiadis[29], M. Vecchi[6], J. Veh[23], C. Venter[9], J. Vink[36], H.J. Völk[2], N. Vogel[23], T. Wach[23], S.J. Wagner[4], F. Werner[2], R. White[2], A. Wierzcholska[26], Yu Wun Wong[23], H. Yassin[9], M. Zacharias[4,9], D. Zargaryan[1], A.A. Zdziarski[34], A. Zech[20], S.J. Zhu[11], A. Zmija[23], S. Zouari[15] and N. Żywucka[9].

[1] Dublin Institute for Advanced Studies, 31 Fitzwilliam Place, Dublin 2, Ireland

[2] Max-Planck-Institut für Kernphysik, P.O. Box 103980, D 69029 Heidelberg, Germany

[3] Yerevan State University, 1 Alek Manukyan St, Yerevan 0025, Armenia

[4] Landessternwarte, Universität Heidelberg, Königstuhl, D 69117 Heidelberg, Germany

[5] IRFU, CEA, Université Paris-Saclay, F-91191 Gif-sur-Yvette, France

[6] Kapteyn Astronomical Institute, University of Groningen, Landleven 12, 9747 AD Groningen, The Netherlands

[7] Laboratoire Leprince-Ringuet, École Polytechnique, CNRS, Institut Polytechnique de Paris, F-91128 Palaiseau, France

[8] University of Namibia, Department of Physics, Private Bag 13301, Windhoek 10005, Namibia

[9] Centre for Space Research, North-West University, Potchefstroom 2520, South Africa

[10] Universität Hamburg, Institut für Experimentalphysik, Luruper Chaussee 149, D 22761 Hamburg, Germany

[11] Deutsches Elektronen-Synchrotron DESY, Platanenallee 6, 15738 Zeuthen, Germany

[12] Obserwatorium Astronomiczne, Uniwersytet Jagielloński, ul. Orla 171, 30-244 Kraków, Poland

[13] Department of Physics, University of the Free State, PO Box 339, Bloemfontein 9300, South Africa

[14] Institut für Physik und Astronomie, Universität Potsdam, Karl-Liebknecht-Strasse 24/25, D 14476 Potsdam, Germany

[15] Université de Paris, CNRS, Astroparticule et Cosmologie, F-75013 Paris, France

[16] Department of Physics and Electrical Engineering, Linnaeus University, 351 95 Växjö, Sweden

[17] School of Physics, University of the Witwatersrand, 1 Jan Smuts Avenue, Braamfontein, Johannesburg, 2050 South Africa

[18] Institut für Physik, Humboldt-Universität zu Berlin, Newtonstr. 15, D 12489 Berlin, Germany

[19] Institut für Astronomie und Astrophysik, Universität Tübingen, Sand 1, D 72076 Tübingen, Germany

[20] Laboratoire Univers et Théories, Observatoire de Paris, Université PSL, CNRS, Université Paris Cité, 5 Pl. Jules Janssen, 92190 Meudon, France

[21] Sorbonne Université, Université Paris Diderot, Sorbonne Paris Cité, CNRS/IN2P3, Laboratoire de Physique Nucléaire et de Hautes Energies, LPNHE, 4 Place Jussieu, F-75252 Paris, France

[22] University of Oxford, Department of Physics, Denys Wilkinson Building, Keble Road, Oxford OX1 3RH, UK

[23] Friedrich-Alexander-Universität Erlangen-Nürnberg, Erlangen Centre for Astroparticle Physics, Nikolaus-Fiebiger-Str. 2, 91058 Erlangen, Germany

[24] Astronomical Observatory, The University of Warsaw, Al. Ujazdowskie 4, 00-478 Warsaw, Poland

[25] Université Savoie Mont Blanc, CNRS, Laboratoire d'Annecy de Physique des Particules - IN2P3, 74000 Annecy, France

[26] Instytut Fizyki Jądrowej PAN, ul. Radzikowskiego 152, 31-342 Kraków, Poland

[27] Université Bordeaux, CNRS, LP2I Bordeaux, UMR 5797, F-33170 Gradignan, France

PoS(ICRC2023)589

[28] School of Physical Sciences, University of Adelaide, Adelaide 5005, Australia

[29] Laboratoire Univers et Particules de Montpellier, Université Montpellier, CNRS/IN2P3, CC 72, Place Eugène Bataillon, F-34095 Montpellier Cedex 5, France

[30] Aix Marseille Université, CNRS/IN2P3, CPPM, Marseille, France

[31] Universität Innsbruck, Institut für Astro- und Teilchenphysik, Technikerstraße 25, 6020 Innsbruck, Austria

[32] Institute of Astronomy, Faculty of Physics, Astronomy and Informatics, Nicolaus Copernicus University, Grudziadzka 5, 87-100 Torun, Poland

[33] Department of Physics, Rikkyo University, 3-34-1 Nishi-Ikebukuro, Toshima-ku, Tokyo 171-8501, Japan

[34] Nicolaus Copernicus Astronomical Center, Polish Academy of Sciences, ul. Bartycka 18, 00-716 Warsaw, Poland

[35] Department of Physics and Astronomy, The University of Leicester, University Road, Leicester, LE1 7RH, United Kingdom

[36] GRAPPA, Anton Pannekoek Institute for Astronomy, University of Amsterdam, Science Park 904, 1098 XH Amsterdam, The Netherlands

[37] Yerevan Physics Institute, 2 Alikhanian Brothers St., 0036 Yerevan, Armenia

[38] Department of Physics, Konan University, 8-9-1 Okamoto, Higashinada, Kobe, Hyogo 658-8501, Japan

[39] Kavli Institute for the Physics and Mathematics of the Universe (WPI), The University of Tokyo Institutes for Advanced Study (UTIAS), The University of Tokyo, 5-1-5 Kashiwa-no-Ha, Kashiwa, Chiba, 277-8583, Japan

[40] RIKEN, 2-1 Hirosawa, Wako, Saitama 351-0198, Japan